European Review for Medical and Pharmacological Sciences 2022; 26: 399-414

Diagnostic performance of LI-RADS in adult patients with rare hepatic tumors

V. GRANATA[1], R. FUSCO[2], S. VENANZIO SETOLA[1], M.L. BARRETTA[1], D.M.A. IASEVOLI[1], R. PALAIA[3], A. BELLI[3], R. PATRONE[3], F. TATANGELO[4], G. GRAZZINI[5], R. GRASSI[6,7], F. GRASSI[6], R. GRASSI[6,7], A. ANSELMO[8], F. IZZO[3], A. PETRILLO[1]

[1]Division of Radiology, "Istituto Nazionale Tumori IRCCS Fondazione Pascale – IRCCS di Napoli", Naples, Italy
[2]Medical Oncology Division, Igea SpA, Naples, Italy
[3]Division of Hepatobiliary Surgical Oncology, "Istituto Nazionale Tumori IRCCS Fondazione Pascale – IRCCS di Napoli", Naples, Italy
[4]Division of Pathology, "Istituto Nazionale Tumori IRCCS Fondazione Pascale – IRCCS di Napoli", Naples, Italy
[5]Division of Radiology, "Azienda Ospedaliero-Universitaria Careggi", Florence, Italy
[6]Division of Radiology, "Università degli Studi della Campania Luigi Vanvitelli", Naples, Italy
[7]Italian Society of Medical and Interventional Radiology (SIRM), SIRM Foundation, Milan, Italy
[8]HPB Surgery and Transplant Unit, Department of Surgery, Policlinico Tor Vergata, Rome, Italy

Abstract. – OBJECTIVE: The rare hepatic tumor can have a wide spectrum of radiologic features, representing a diagnostic challenge. Our purpose is to report the experience of a National Cancer Center, emphasizing the radiological features encountered and assessing the LR-M categories in the diagnostic performances for these lesions.

PATIENTS AND METHODS: We assessed 113 patients who underwent surgical resection or biopsy for rare liver lesions from May 2010 to December 2020. For these patients a computerized search of radiological records was performed to identify which had been studied with MRI and CT. For each lesion, the radiologists recorded the attenuation on CT studies and signal intensity (SI) in T1 weighted (W), in T2-W, DWI and in the related map of the apparent diffusion coefficient (ADC). We assessed the presence and the type of contrast enhancement (CE) during contrast study on CT and MRI and the enhancement was categorized according to LI-RADS 2018. We also assessed the presence of other features in LR-M categories (ancillary LR-M features) in order to classify different subgroups.

The lesions were classified according to LR categories, and the gold standard was histological analysis.

RESULTS: The final study population included 95 patients (46 females and 49 males), with a mean age of 51 years (range 38-83 years). 83 patients had solid lesions, 12 patients had cystic lesions (simple or complex). According to histological analysis, we categorized 79 patients with malignant lesions and 16 patients with benign lesions. According to radiological features we assessed as malignant 82 patients (79 true malignant and 3 false malignant), as benign 13 patients (all true benign). Therefore, sensitivity, specificity, positive predictive value, negative predictive value and accuracy of radiological features to identify benign and malignant lesions were 100.0%, 81.3%, 96.3%, 100.0% and 96.8%, respectively. We found no significant difference in signal and contrast enhancement appearance among all LR-M categories (p-value =0.34 at Chi square test). However, among LR-M categories the presence of satellite nodules was a feature typical of cHCC-CC (*p*-value < 0.05 at Chi square test). The presence of intra lesion necrosis and haemorrhage was suggestive of sarcoma (*p*-value < 0.05 at Chi square test).

CONCLUSIONS: High diagnostic accuracy was obtained by LI-RADS classification between malignant and benign lesion. The presence of ancillary features could help the radiologist towards a correct diagnosis.

Key Words:
Rare hepatic tumor, LI-RADS, Magnetic resonance imaging, Computed tomography.

Introduction

The neoplasms of the liver include primary lesions and metastases. Moreover, a wide spec-

Corresponding Author: Vincenza Granata, MD; e-mail: v.granata@istitutotumori.na.it

trum of benign and malignant tumors may develop[1]. Among the malignant neoplasm Hepatocellular carcinoma (HCC) and cholangiocarcinoma (CC) are the most common while among the benign lesions hepatic angioma is the most frequent with a wide literature reporting their radiological features[2-10]; however, there are other types of tumors, with inadequate literature, with radiological features that the radiologists often confuse with those of the most common lesions, but which require different treatments[11-16]. Rare primary hepatic tumor can be classified according to their cell of origin as shown in Table I. Rare primary liver lesions are cathegorized as cystic or solid by their structure and as intra parenchymal or extra parenchymal considering their anatomical site. The radiologic features knowledge of the various liver tumours is essential in the correct diagnosis and management of these tumors[17]. The clinical history often does not help in the diagnosis as these patients may be asymptomatic or paucisymptomatic[1] and the diagnosis in some cases can be accidental. Ultrasound (US), Computed Tomography (CT) and Magnetic Resonance (MR) are the diagnostic tools used to assess liver disease in the diagnosis, staging and follow-up providing also information to guide the clinician *vs.* the surgical resectability or *vs.* a loco regional treatment[18-20]. Although US is, occasionally, the primary tool considered in the liver assessment, its accuracy varies according to operator experience. The US accuracy is lower than CT and MRI accuracy to estimate tumour spread and resectability[21,22]. CT and MRI are imaging modalities with multiplanar capability to assess liver lesions. MRI provides morphological and functional data of different tumours and functional data of residual liver parenchymal. For these reasons, MRI is the preferred imaging tool for patients with suspected liver tumours[23-32].

Table I. The effect of liraglutide and methotrexate on biochemical markers and body weight change in MTX induced cardiotoxicity in rats.

Epithelial tumors
- Benign:
  - Hepatocellular adenoma
  - Focal nodular hyperplasia
  - Intrahepatic bile duct adenoma
  - Intrahepatic bile duct cystadenoma
  - Biliary papillomatosis
- Malignant:
  - Hepatocellular carcinoma
  - Intrahepatic cholangiocarcinoma
  - Bile duct cystadenocarcinoma
  - Combined hepatocellular and cholangiocarcinoma
  - Hepatoblastoma
  - Undifferentiated carcinoma

Non-epithelial tumors
- Benign:
  - Angiomyolipoma
  - Lymphangioma and lymphangiomatosis
  - Hemangioma
  - Infantile hemangioendothelioma
- Malignant:
  - Epithelioid hemangioendothelioma
  - Angiosarcoma
  - Embryonal sarcoma
  - Rhabdomyosarcoma
  - Others

Miscellaneous tumors
- Solitary fibrous tumor
- Teratoma
- York sac tumor
- Carcinosarcoma
- Rhabdoid tumor
- Others

Hematopoietic and lymphoid tumors
Secondary tumors
Epithelial abnormalities
- Liver cell dysplasia
- Dysplastic nodules
- Bile duct abnormalities

Miscellaneous lesions
- Mesenchymal hamartoma
- Nodular transformation
- Inflammatory pseudotumor

The Liver Imaging Reporting and Data System (LI-RADS) was developed to improve consistency and clarity of communication among radiologists and clinician about liver imaging findings. LI-RADS is widely used for HCC non-invasive diagnosis and was recently used in the Practice Guidance from the American Association for the Study of Liver Diseases. However, this system is appropriate in patients who have both chronic liver disease (either cirrhosis or chronic hepatitis) and a history of extrahepatic primary malignancy while the LI-RADS performance is not tested in the assessment of other liver neoplasm. A recent study[17] repported a comparative and comprehensive analysis of imaging findings of rare liver tumours. The objective of this study is to report the experience of a National Cancer Center of Naples in the diagnostic performances for rare hepatic tumors emphasizing the radiological features encountered using the LR-M categories.

Patients and Methods

Patient Population

Local Ethical Committee of National Cancer Institue of Naples approved this retrospective study and waived the requirement for informed

consent. Patients subjected to surgical resection or biopsy for rare liver lesions from May 2010 to December 2020 were identified. The patients with confirmed histological diagnosis of hepatic rare tumors were enrolled. Final study population included 113 patients. Moreover, a new computerized search of radiological records was performed to identify the patients that had been studied with MRI and CT.

MR Imaging Protocol

1.5T MR scanner (Magnetom Symphony, with Total Imaging Matrix Package, Siemens, Erlangen, Germany) with 8-element body and phased array coils was used to acquire MRI. MRI included basal images taken before contrast medium administration and then functional dynamic sequences obtained after IV injection of liver-specific contrast medium, acquiring the last series of images with a delay of 20 min during the hepatobiliary excretion. After the IV injection, VIBE T1-weighted FS (SPAIR) sequences were acquired in four different phases: hepatic arterial- (35 s delay), portal venous- (90 s), transitional- (120 s) and hepatobiliary excretion phase (20 min).

The liver-specific gadolinium was administrated at each patient according to our previous study[17].

In Table II we reported MRI study protocol.

CT Protocol

64-detector row scanner (Optima 660, GE Healthcare, US) was used to acquire the liver CT study. CT scanning parameters were 120 kVp, 100-470 mAs (NI 16.36), 2.5-mm slice thickness and table speed 0.984/1 mm/rotation. Liver protocol examinations were composed of quadruple phases: unenhanced, arterial, portal venous, and equilibrium phases. CT images were obtained for each patient according to our previous study[17].

Images Analysis

Expert radiologists in liver imaging reviewed in consensus MR and CT studies. reviewed in consensus MR and CT studies. The radiologists classified the lesions as intraparenchymal or extra parenchymal/peribiliary considering their site and as cystic (simple or complex, with a partial solid component) or solid considering their structure[29,31]. The lesions maximum diameter was measured on T1 weighted (W), T2 W, portal phase VIBE T1 W, hepatobiliary-phase VIBE T1 W and CT portal phase. For each lesion, the radiologists recorded the attenuation on CT scan and signal intensity (SI) in T1 W, T2-W, DWI and in the apparent diffusion coefficient (ADC) map. The CT attenuation was classified as isodense, hypodense and hyperdense compared with surrounding liver parenchyma. The SI was classified as isointense, hypointense or hyperintense. ADC median value was calculated as representative value for each region of interest on the liver lesion drawn by radiologists[17].

These features were assessed also according to LI-RADS to identify the categories for each one[33,34].

We assessed the presence and the type of contrast enhancement (CE) during arterial, portal, transitional and hepatobiliary phase on MR study; during the arterial, portal, late phase on CT study.

The enhancement was categorized according to LI-RADS 2018, as reported in Table III[33,34].

We also assessed the presence of other features in LR-M categories (ancillary LR-M features) in order to classify different subgroups.

The lesions were classified according to LR categories, and the gold standard was histological analysis.

If a patient had multiple lesions satisfying inclusion criteria, the largest lesion was selected for

Table II. MR acquisition protocol.

Sequence	Orientation	TR/TE/FA (ms/ms/deg.)	AT (min)	Acquisition Matrix	ST/Gap (mm)	FS
Trufisp T2-W	Coronal	4.30/2.15/80	0.46	512x512	4 / 0	without
HASTE T2-W	Axial	1500/90/170	0.36	320x320	5 / 0	Without and with (SPAIR)
HASTE T2w	Coronal	1500/92/170	0.38	320x320	5 / 0	without
SPACE T2W FS	Axial	4471/259/120	4.20	384x450	3/0	With (Spair)
In-Out phase T1-W	Axial	160/2.35/70	0.33	256x192	5 / 0	without
DWI	Axial	7500/91/90	7	192x192	3 / 0	without
Vibe T1-W	Axial	4.80/1.76/12	0.18	320x260	3 / 0	with (SPAIR)

Note. TR = Repetition time, TE = Echo time, FA = Flip angle, AT = Acquisition time, ST = Slice thickness, FS= Fat suppression, SPAIR = Spectral adiabatic inversion recovery.

Table III. Term, definition, Comment, Data Approved, Synonyms of LR-M observation to assess hepatic lesion.

Term	Definition	Comment	Date Approved	Synonyms	Type of term	Applicable modalities
Targetoid	Target-like imaging morphology. The center and periphery of a mass have different imaging characteristics.	The presence of targetoid appearance suggests iCCA or other non-HCC malignancy, but it does not exclude HCC.	11/2019	Target-like, target appearance	Imaging feature, LR-M	CT, MRI
Rim arterial phase hyperenhancement (rim APHE)	Subtype of APHE in which arterial phase enhancement is most pronounced in observation periphery. Rim APHE is a subtype of targetoid morphology.	The presence of rim APHE suggests iCCA or other non-HCC malignancy, but it does not exclude HCC. Rim APHE can be smooth or irregular. It can vary in thickness.	11/2019	Peripheral APHE, ring APHE, targetoid APHE, APHE in target pattern, rim enhancement	Imaging feature, LR-M	CEUS, CT, MRI
Peripheral washout appearance (peripheral "washout")	Subtype of "washout" in which apparent washout is most pronounced in observation periphery. Peripheral "washout" is a subtype of targetoid morphology.	presence of peripheral "washout" suggests iCCA or other non-HCC malignancy, but it does not exclude HCC.	11/2019	Peripheral washout; venous/portal venous/delayed/late phase peripheral hypoenhancement, peripheral hypoattenuation, or hypointensity; peripheral deenhancement	Imaging feature, LR-M	CT, MRI
Delayed central enhancement	Area of postarterial phase enhancement most pronounced in the inside rather than in the periphery of the lesion. Delayed central enhancement is a subtype of targetoid morphology. The area of delayed enhancement in a lesion may be central, eccentric, or heterogeneous, but not peripheral.	The presence of delayed central enhancement suggests iCCA or other non-HCC malignancy, but it does not exclude HCC.	11/2019	Sustained central enhancement, concentric progressive enhancement, centripetal progressive enhancement	Imaging feature, LR-M	CT, MRI
Targetoid restriction	Concentric pattern on DWI characterized by restricted diffusion in observation periphery with less restricted diffusion in observation center.	The presence of targetoid restriction suggests iCCA or other non-HCC malignancy, but it does not exclude HCC.	11/2019	Peripheral restriction, DWI target sign/appearance, targetoid diffusion	Imaging feature, LR-M	MRI
Targetoid transitional phase (TP) or hepatobiliary phase (HBP) appearance	Concentric pattern in TP or HBP characterized by moderate-to-marked hypointensity in observation periphery with milder hypointensity in center.	The presence of targetoid TP or HBP appearance suggests iCCA or other non- HCC malignancy, but it does not exclude HCC.	11/2019	HBP/TP cloud, HBP/TP target sign/appearance	Imaging feature, LR-M	MRI

evaluation and when more features were present the predominant one was chosen as target.

Statistical Analysis

To analyse differences in percentage values of categorical variable, the Chi-square test was used while the Kruskal-Wallis test was used to identify differences between the median values of the continuous variables.

A p-value < 0.05 was considered as statistically significant.

Statistical analysis was obtained by means of the Statistic Toolbox of Matlab (The MathWorks, Inc., Natick, MA, USA).

Results

The final study population included 95 patients (46 females and 49 males), with a mean age of 51 years (range 38-83 years). 83 patients had solid lesions, 12 patients had cystic lesions (simple or complex). We excluded 18 patients due to the absence of in-MR and in-CT examination.

Among solid lesions we assessed:

- 46 patients with peribiliary metastases (21 Men - 25 Women; median age 62 y; range 40-83: 21 patients with CRC, 7 with pancreatic cancer, 7 with breast cancer, 5 with gastric cancer, 1 with endometrial cancer, 3 with ovarian cancer had biliary metastases, 2 with neuroendocrine tumor).
- 18 patients with cHCC-CCA (7 Women - 11 Men; mean age 67; range 48-82), with a single active lesion (mean size 42.0 mm (range 23-80 mm). All patients were classified as Child-Pugh class A (8 with chronic hepatitis B and 10 with chronic hepatitis C) (Figure 1).
- 3 patients with non-typical HCC: 1 patient had HCC in non-cirrhotic liver; 1 patient had fibrolamellar HCC and 1 patient had primary clear cell carcinoma.
- 1 patient had hepatic adenomatosis (Figure 2).

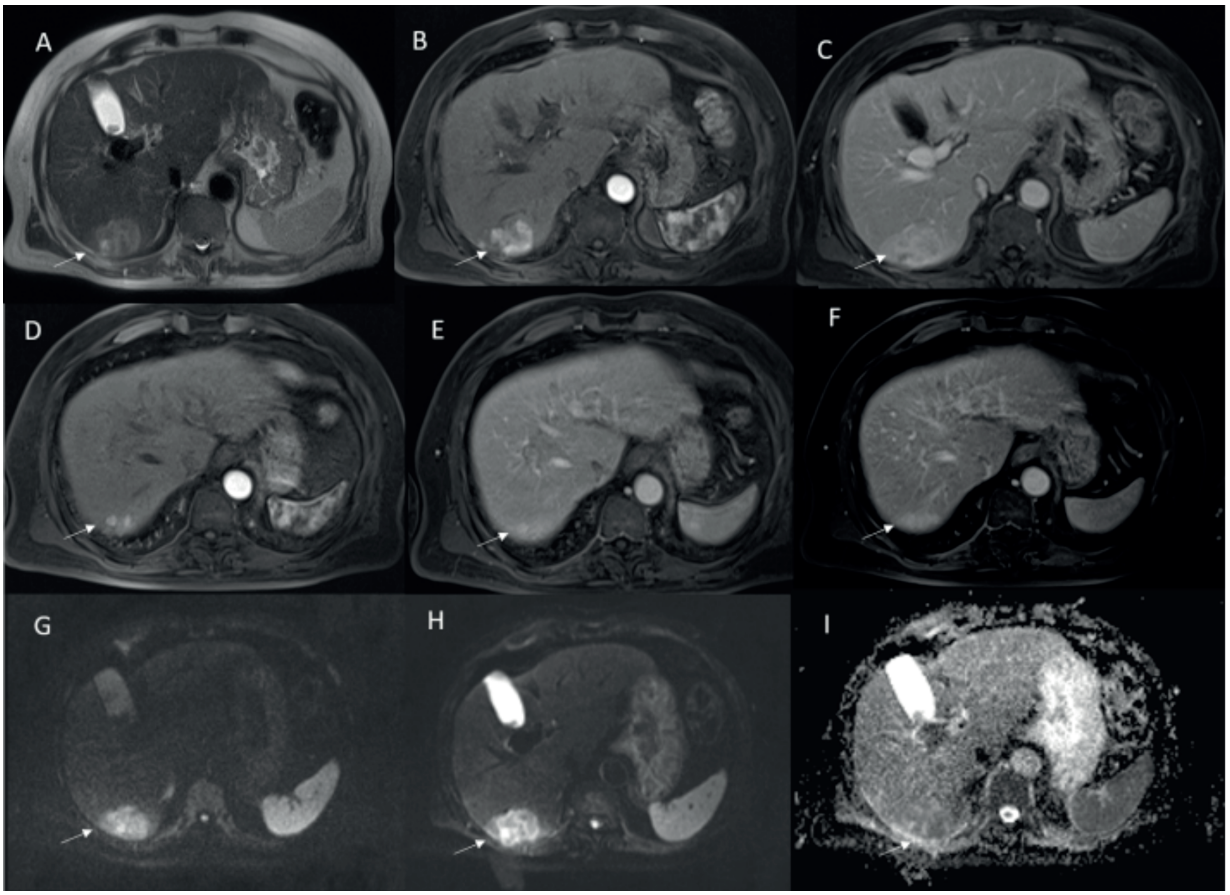

Figure 1. cHCC-CCA patient. The lesion shows (arrow) targetoid appearance in T2-W sequences (**A**), APHE in arterial phase (**B**) and non peripheral wash-out appearance in portal phase (**C**). In **D**, **E** and **F**, the arrow shows satellite nodules. In DWI sequences (**G**, **H**) and ADC map the lesion shows restricted diffusion **(I)**.

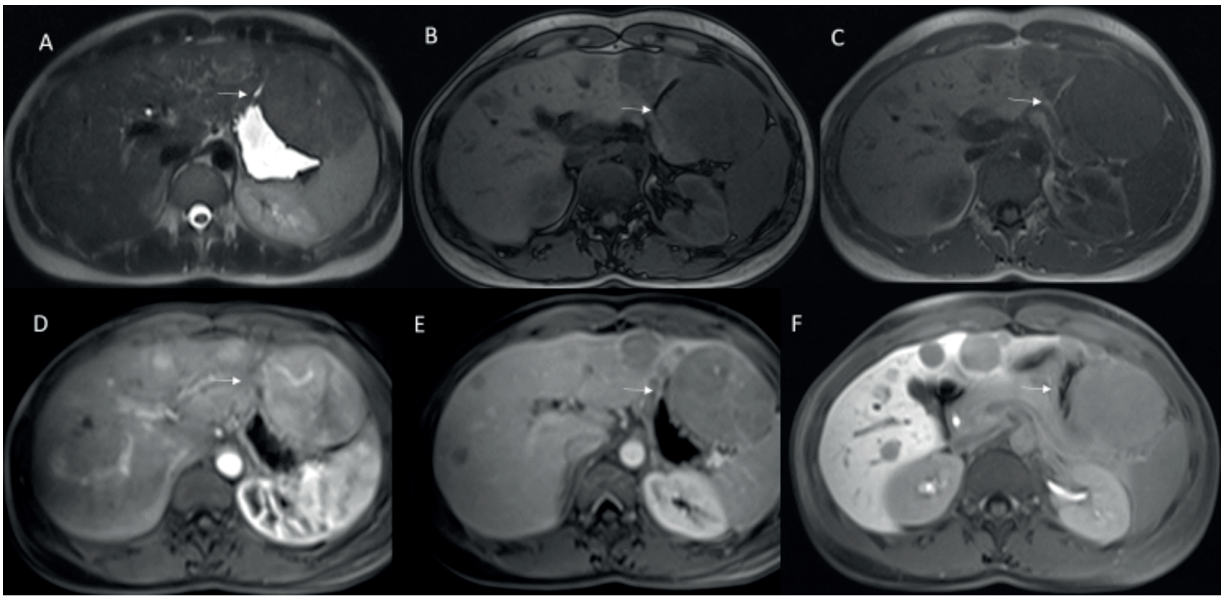

Figure 2. Hepatic Adenomatosis. The arrow shows the lesion that appears iso-hyperintense in T2-W (**A**), hypointense in T1-W sequences (**B**: out of phase; **C**: in phase). During contrast study, the lesion shows APHE in arterial phase (**D**), wash-out appearance in portal phase (**E**) and hypointense signal in HB phase (**F**).

- 3 patients had primary hepatic NET (Figure 3).
- 4 patients had hepatic lymphoma.
- 2 patients had lesions due to oxaliplatin (Figure 4).
- 1 patient had primary hepatic melanoma (Figure 5).
- 1 patient had biliary adenoma.
- 2 patients had necrotic solitary nodule.
- 1 patient had angiosarcoma.
- 1 patient had primary hepatic carcinosarcoma (Figure 6).

Among cystic lesions, we assessed:

- ˆ4 patients with intraductal papillary neoplasm of bile duct (BT-IPNB) (Figure 7).
- 1 patient with degenerated BT-IPNB (Figure 8).
- 6 patients had cystadenoma (Figure 9).
- 1 patient had cystadenocarcinoma (Figure 10).

According to histological analysis, we categorized 79 patients with malignant lesions and 16 patients with benign lesions (included hepatic adenomatosis and BT-IPNB).

Ninety-four patients underwent MR study (excluded patients with angiosarcoma) and 75 patients underwent CT study (46 patients with biliary metastases, 18 with cHCC-CCA, 3 patients with non-typical HCC, 2 patients with Net, 2 with lesions to oxaliplatin, 1 with melanoma, 1 with degenerated IPNB, 2 with lymphoma).

Imaging Features

Lesion size ranged between 15 and 230 mm (medium value of 47 mm). No difference statistically significant was found in the diameters of the lesions measured on CT and MR images (p-value = 0.23 at Kruskal Wallis test).

According to lesions anatomical site, we identified 41 intra parenchymal lesions and 54 intraparenchymal/peribiliary lesions. Among the cystic lesions, the lesion was simple in 10 cases (4 patients with BT-IPNB and 6 with cystadenoma). Signal intensity on T1 W and T2 W images appeared similar to that of the gallbladder. The lesion showed a not very restricted diffusion and iso-hyperintense SI on ADC map. According to LI-RADS categories, we identified these lesions as benign.

In two patients with complex cystic lesion, (one with cystadenocarcinoma and another with degenerated IPNB), the cystic component was combined with a solid one showing heterogeneously hypointense on T1 W images and hyperintense on T2 W images. The solid portion had restricted diffusion with hypointense targetoid SI on ADC map. The solid component showed heterogeneous CE on CT and MR images, with a progressive CE during different phase of study. According to LI-RADS categories, we classified these lesions as LR-M. The cystic component was assessed as an ancillary LR-M feature. In addition, in patients with degenerated IPNB, the infiltrative appearance and the presence of biliary dilatation were documented as ancillary LR-M features.

Among the patients with solid lesions, we identified as LR-1 categories 3 subjects (2 with necrotic

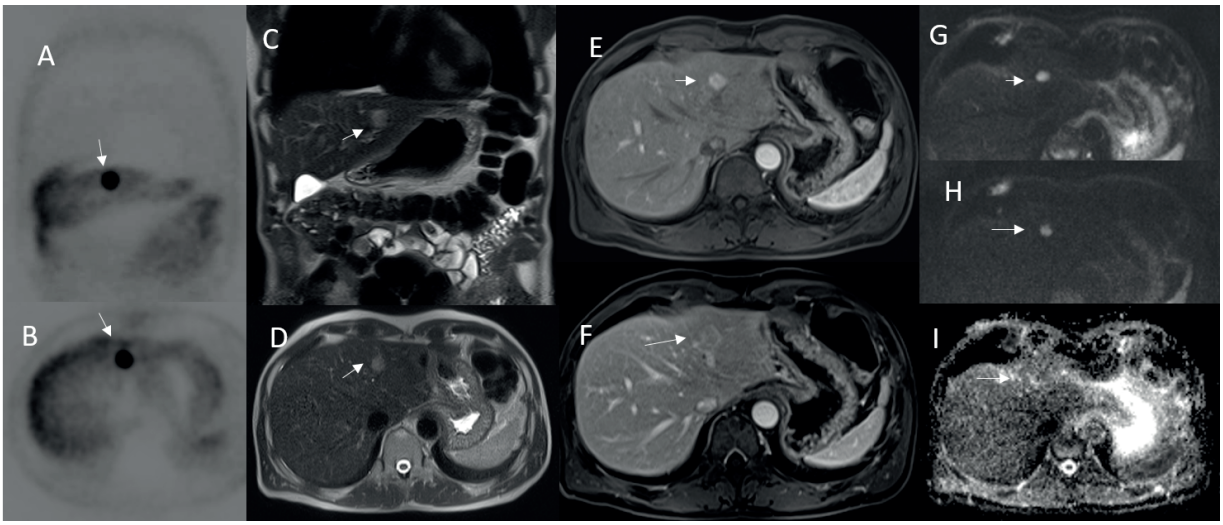

Figure 3. Hepatic NET. The nodule is detected (arrow) by 68Ga-DOTATOC-PET/CT (**A** and **B**), showing hyperintense signal (arrow) in T2-W sequences (**C** and **D**). The lesion shows hypervascular appearance (arrow) during arterial phase (**E**) and "peripheral rim" (arrow) during portal phase (**F**) of contrast study, with restricted diffusion (**G**, **H** and **I**).

nodule and one with biliary adenoma). In these patients the SI was hypointense in T1 W sequences, iso-hypointense in T2 W sequences; diffusion was not restricted, and the SI was isointense on ADC map. No contrast enhancement was present in these lesions.

We classified as LR-M the 2 patients with oxaliplatin lesions. The lesions showed SI hypointense on T1 W sequences, hyperintense on T2 W sequences, restricted diffusion with isointense SI on ADC map. During contrast study the lesions showed heterogeneous CE, many of these showed

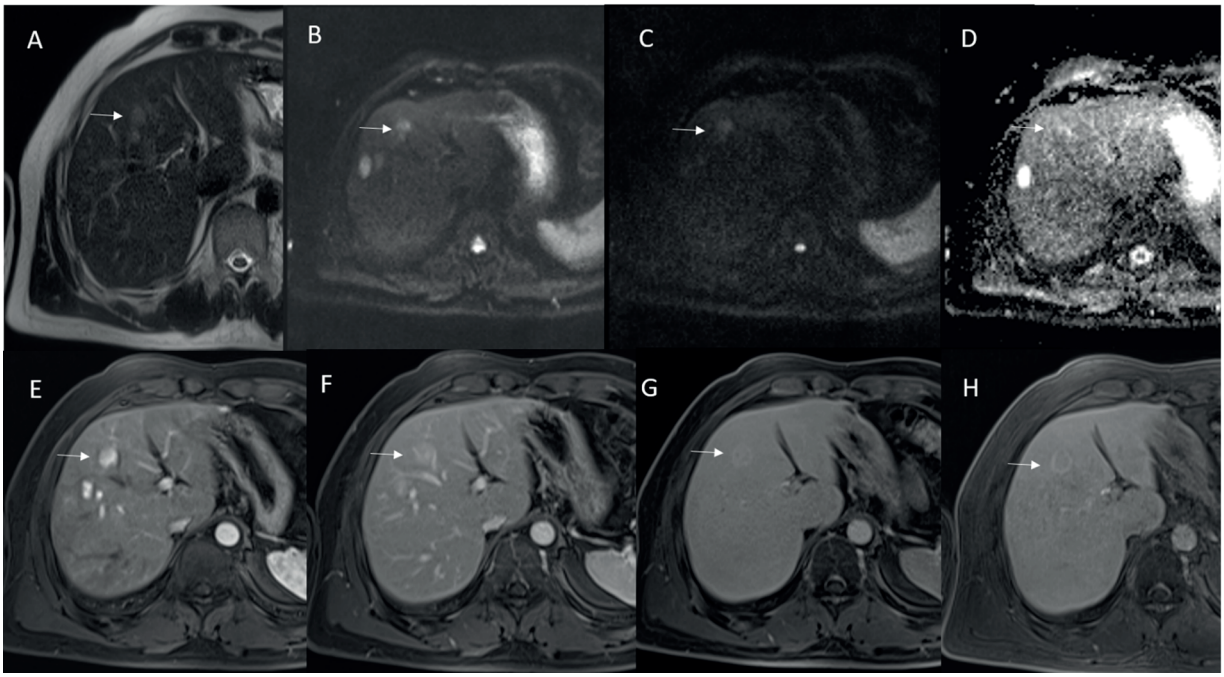

Figure 4. Lesion due to oxaliplatin. The lesion shows hypointense SI in T2-W (**A**), with restricted diffusion (**B**, **C** and **D**). During contrast study, the lesion shows APHE in arterial phase (**E**), hypointense SI in portal phase (**F**), with peripheral rim APHE in transitional (**G**) and HB phase (**H**).

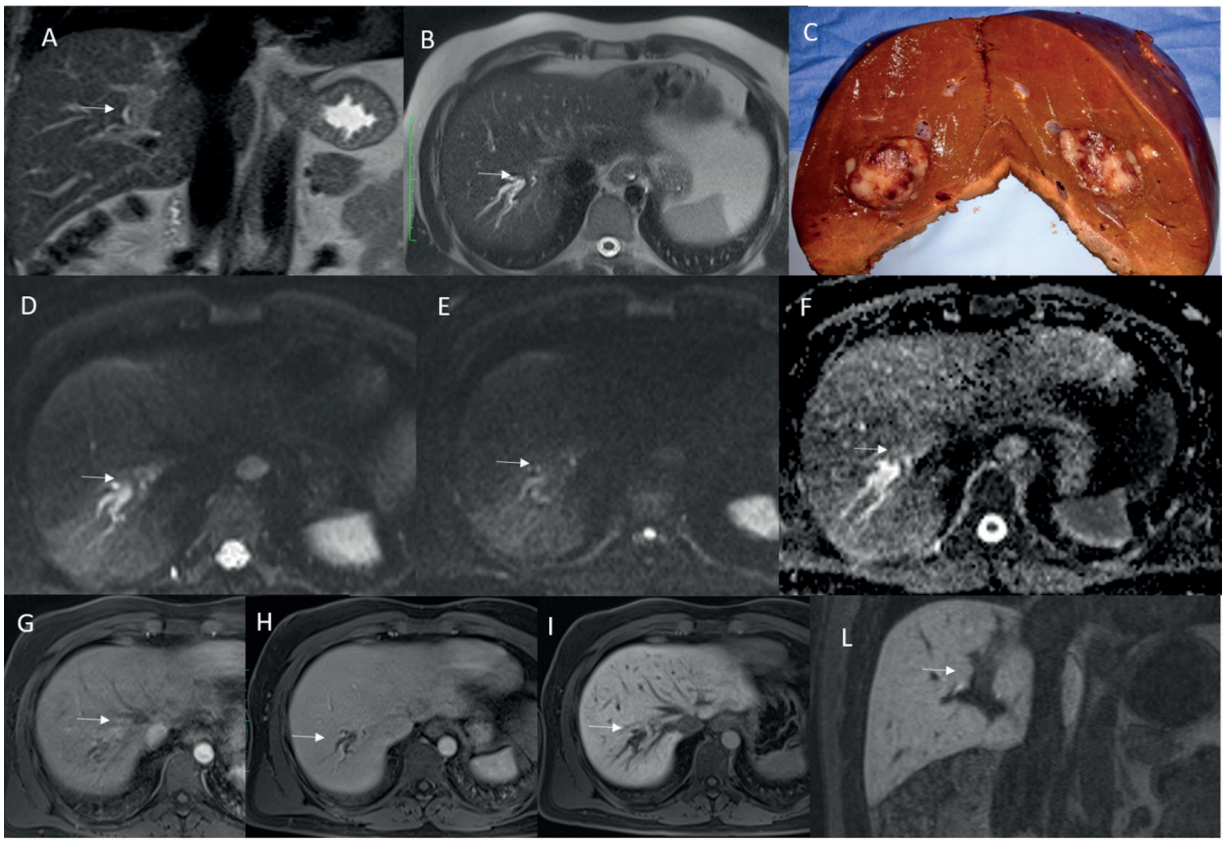

Figure 5. Hepatic melanoma. The lesion shows hyperintense SI (arrow) in T2-W sequences (**A** and **B**), with biliary dilatation. In **C** it is shown specimen. The lesion shows restricted diffusion (**D** and **E**: b800 s/mm^2) with hypointense SI in ADC map (**F**). During contrast study the lesion shows progressive contrast enhancement (**G**: arterial phase; **H**: portal phase), with hypointense SI in HB phase (**I** and **L**).

arterial phase hyperenhancement (APHE), isointense signal on portal and transitional phase and peripheral hyperintense rim during hepatospecific phase (HBP) with a targetoid appearance.

We classified as LR-5 8 patients: 5 with cHCC-CC, 2 patients with non-typical HCC (1 with HCC in non-cirrhotic liver and 1 patient with primary clear cell carcinoma) and 1 patient with hepatic adenomatosis. The lesions showed SI hypointense in T1 W, hyperintense in T2 W, restricted diffusion with hypointense SI on ADC map. During contrast study, the lesions showed APHE, washout and capsule appearance with hypointense signal on HBP phase.

Thirteen patients with cHCC-CC and 1 with fibrolamellar HCC were classified as LR-M, showing rim APHE, non-peripheral washout appearance and a progressive CE with targetoid appearance in HBP. The SI was inhomogeneous hyperintense in T2 W, inhomogeneous hypointense in T1-W sequences, with targetoid appearance in b800 s/mm^2 and in ADC map.

All cHCC-CC patients had satellite nodules. The absence of the pseudo-capsule, progressive CE and satellite nodules showed percentages statistically different in cHCC-CC (p-value <0.01 at Chi square test) compared to others LR-M categories.

The three patients with primitive NET were classified as LR-4. The lesions showed SI hypointense on T1 W sequences, hyperintense on T2 W sequences, restricted diffusion with hypointense SI on ADC map. During contrast study, the lesions showed APHE, isointense SI in portal phase, in one case a rim enhancement, and hypointense signal on HBP phase. No ancillary LR-M features were found in this group.

Among patients with peribiliary lesions (all patients with biliary metastases, 2 patients with lymphoma, 1 patient with hepatic melanoma), the lesions showed hypointense SI in T1 W sequences, hyperintense signal in T2 W sequences. Restricted diffusion with hypointense signal in ADC map. During the contrast-enhanced study,

the lesions showed progressive CE and hypointense SI in HB phase.

The patients with sarcoma (1 patient with angiosarcoma and 1 patient with carcinosarcoma) were cathegorized as LR-M. The lesions showed inhomogeneous hypointense SI in T1 W sequences, inhomogeneous hyperintense signal in T2 W sequences. Progressive CE during the different phase of contrast study. Targetoid appearance in DWI, ADC map and HB phase. In this group the inhomogeneous signal in T1-W and T2-W sequences so as the targetoid appearance in DWI sequences and HB phase were correlated to intra lesion necrosis and haemorrhage that were recorded as ancillary LR-M features.

The remaining solid lesions intraparenchymal lesions (2 patients with lymphoma) were classified as LR-M. The lesions showed hypointense SI in T1 W sequences, hyperintense signal in T2 W sequences. During contrast study, the lesions showed APHE, progressive CE during the different contrast phases and hypointense SI during HB phase. The lesions showed restricted diffusion and hypointense SI in ADC map.

According to radiological features we assessed as malignant 82 patients (79 true malignant and 3 false malignant), as benign 13 patients (all true benign). Therefore, sensitivity, specificity, positive predictive value, negative predictive value and accuracy of radiological features to identify benign and malignant lesions were 100.0%, 81.3%, 96.3%, 100.0% and 96.8%, respectively.

We found no significant difference in signal and CE appearance among all LR-M categories (p-value =0.34 at Chi square test).

However, among LR-M categories the presence of satellite nodules was a feature typical of cHCC-CC (p-value < 0.05 at Chi square test). The presence of intra lesion necrosis and haemorrhage was suggestive of sarcoma (p-value < 0.05 at Chi square test).

Discussion

The Liver Imaging Reporting and Data System (LI- RADS) developed by the American College of Radiology is widely used for non-invasive diagnosis of HCC[33,34]. Recently this system is applicable in patients who have both chronic liver disease and a history of extrahepatic primary malignancy[35]. Several researchers[36-40] have assessed the LI-RADS diagnostic performance in patients not included in the LI-RADS 'high-risk' population.

LI-RADS was developed to improve communication between radiologists and referring clinicians caring for patients at risk for HCC. Although

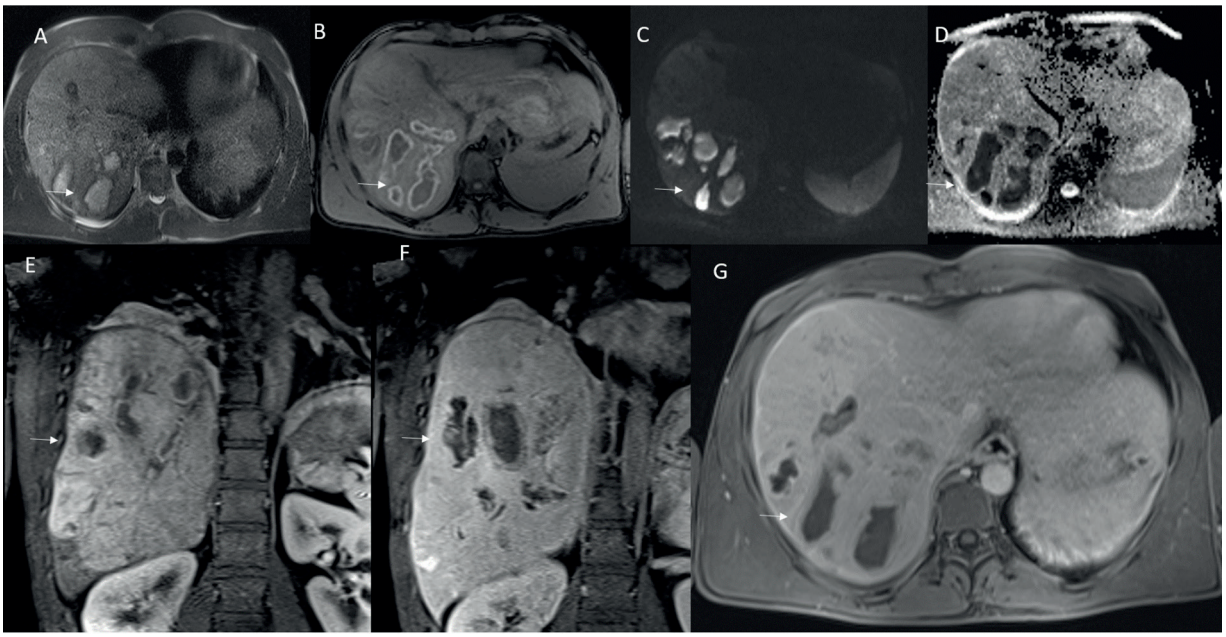

Figure 6. Carcinosarcoma. The lesion shows inhomogeneous hyperintense signal in T2 W sequence (**A**) and inhomogeneous hypointense SI in T1-W sequence (**B**) due to intra lesion necrosis and haemorrhage (arrow), with progressive contrast enhancement during the different phase of contrast study (**E**= arterial, **F** and **G**= portal). Targetoid appearance in DWI (**C**) and ADC map (**D**).

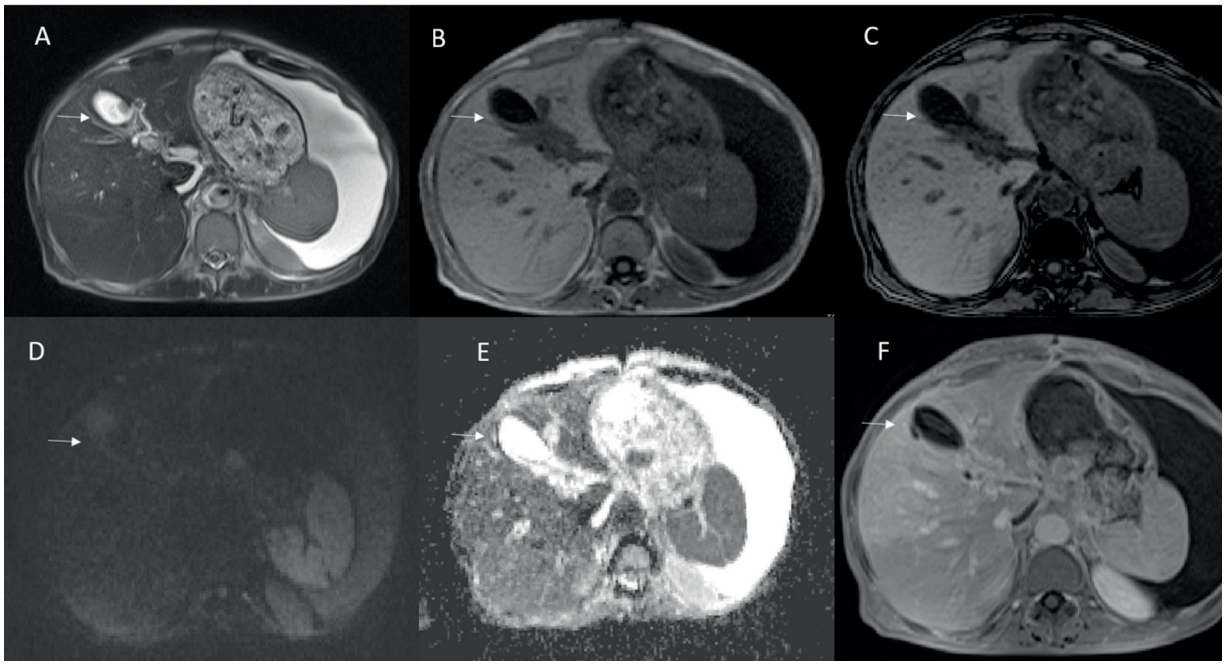

Figure 7. BT-IPNB. It showed hyperintense SI in T2 W images (**A**), communicating with biliary tree, and hypointense SI in T1 W images (**B** and **C**). The lesion showed a no very restricted diffusion (**D**) and hyperintense SI in ADC map (**E**). The lesion shows no contrast enhancement (**F**: portal phase).

the diagnosis of some lesions is exclusive for pathologists, the possibility of identifying a lesion as malignant improves the management of those patients who cannot undergo biopsy. In LI-RADS v2017 was introduced LR-M category (Definite or Probably Malignancy) for non-HCC lesion.

HCC treatment was traditionally based on surgical or loco-regional ablation tecnique. However, HCC is a solid tumor with a highest vascularization; therefore, angiogenesis inhibitor could play an important role in the pharmacological therapeutic approach. Some imaging features could favour a diagnosis of malignancy increasing the CT and MRI diagnostic performance and allowing the stratification of patients who should be treated compared to those who should not be treated[41]. To the best of our knowledge, this is the first work evaluating the LI-RADS diagnostic performance in the assessment of primary hepatic rare tumors in patients not at risk for HCC. We observed, in our population, that LI-RADS has low capability to identify border-line lesions as BT-IPNB and hepatic adenomatosis so as for benign lesions due to oxaliplatin.

BT-IPMN is defined as a papillary mucinous lesion. Four histological subtypes are known (gastric, intestinal, biliopancreatic and oncocytic). It is a rare entity, which can include both the intrahepatic and extrahepatic bile ducts, representing tubular adenocarcinoma or mucinous carcinoma precursor. The malignant degeneration probability for BT-IPMN is high (64-89%), so that the treatment of choice is liver resection. The features to be considered for a correct diagnosis is mucobilia, dilated ducts, shape, enhancement and the mural nodules metabolic activity[17]. However, these features are not included in the LR-M features, and therefore this explains the limitations of these criteria for a correct characterization of these lesions. The majority of malignant BT-IPMN forms have wall nodules with contrast enhancement or solid component that infiltrates the adjacent liver parenchyma. The progressive CE and the targetoid appearance allow identifying as malignant the degenerated BT-IPMN, so as the infiltrative appearance and the cystic component of a lesion.

Hepatic adenomatosis (HA) refers to cases where more than 10 adenomas were present in a normal liver. HA has an incidence of 10-24% in patients with hepatic adenoma, and approximately half the cases are detected incidentally. Today, due to potential for malignant transformation and/or bleeding, treatment of choice is surgical resection, or when it is impractical, liver transplantation. Although this entity might have a malignant transformation, it is a benign lesion and so in our

study LIRADS features did not allow the correct characterization of this lesion[40].

Oxaliplatin chemotherapic drug was administered to patients with metastatic colorectal cancer, and it is responsible for liver sinusoids damage. The damage can determine the solid lesions formation and the differential diagnosis with metastatic lesions remains a challenge. Although in HB phase contrast study, the lesions are isointense with a hyperintense rim or hyperintense; however, the hypodense appearance mimicking metastatic lesions is also reported. According to our results, we classified these lesions as LR-M. Therefore, no ancillary features up today allow to correctly identify these lesions as benign.

Using LIRADS, we classified patient with NET diagnosis as probably HCC due to dynamic contrast studies appearance. Primary hepatic NETS (PHNETs) are extremely rare. In case of NET in the liver, attention must be reserved to exclude metastasis from an extrahepatic unknown site[41] because more than 80% of the liver NETs are metastatic. The radiologic findings of PHNETs have not been well defined, but the cases reported show that the lesions are typically solid[41].

All peribiliary metastases, in our population, were identified as malignant (LR-M). Peribiliary metastases are extremely rare[29,30]. However, in our previous study, we found the percentage of patients with peribiliary metastases to be not low, probably due to the limited value of CT in biliary system tumors diagnosis[30]. We believe that this is linked to the typical progressive CE of peribiliary lesions. Consequently, small lesions can be undetected due to the similar signal attenuation compared to surrounding parenchyma. For larger lesions, the indirect sign as biliary ducts dilatation could help to identify the tumor. MRI could detect all metastases, with the best perfor-

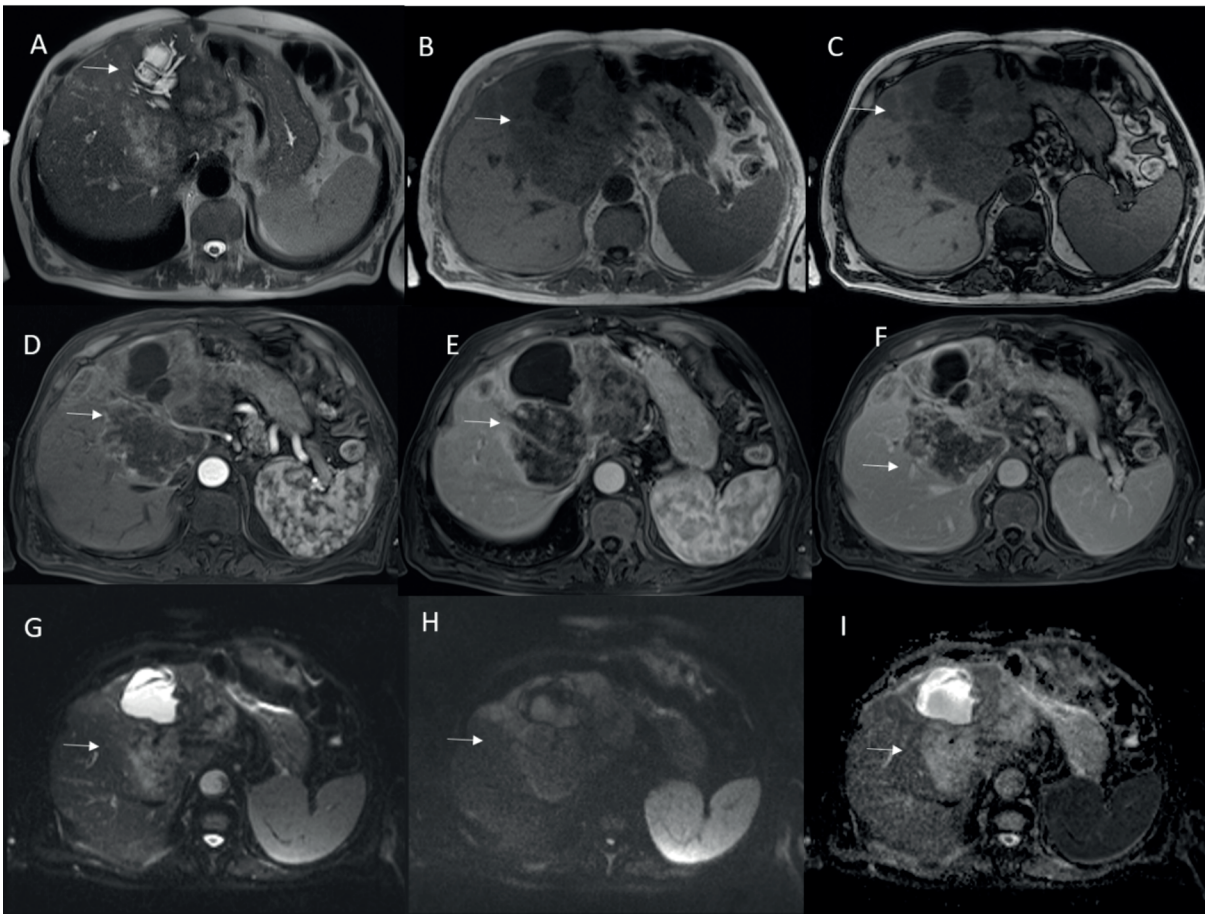

Figure 8. Degenerated BT-IPMN. The solid component that infiltrates the adjacent liver parenchyma shows targetoid appearance in T2-W sequence (**A**), hypointense SI in T1 (**B**: in phase and **C**: out ph phase sequence) with progressive contrast enhancement during contrast study (**D**: arterial, **E**: late arterial and **F**: portal phase) with targetoid appearance in DWI sequences (**G**: b 50 s/mm^2 and **H**: b 800 s/mm^2) and ADC map (**I**).

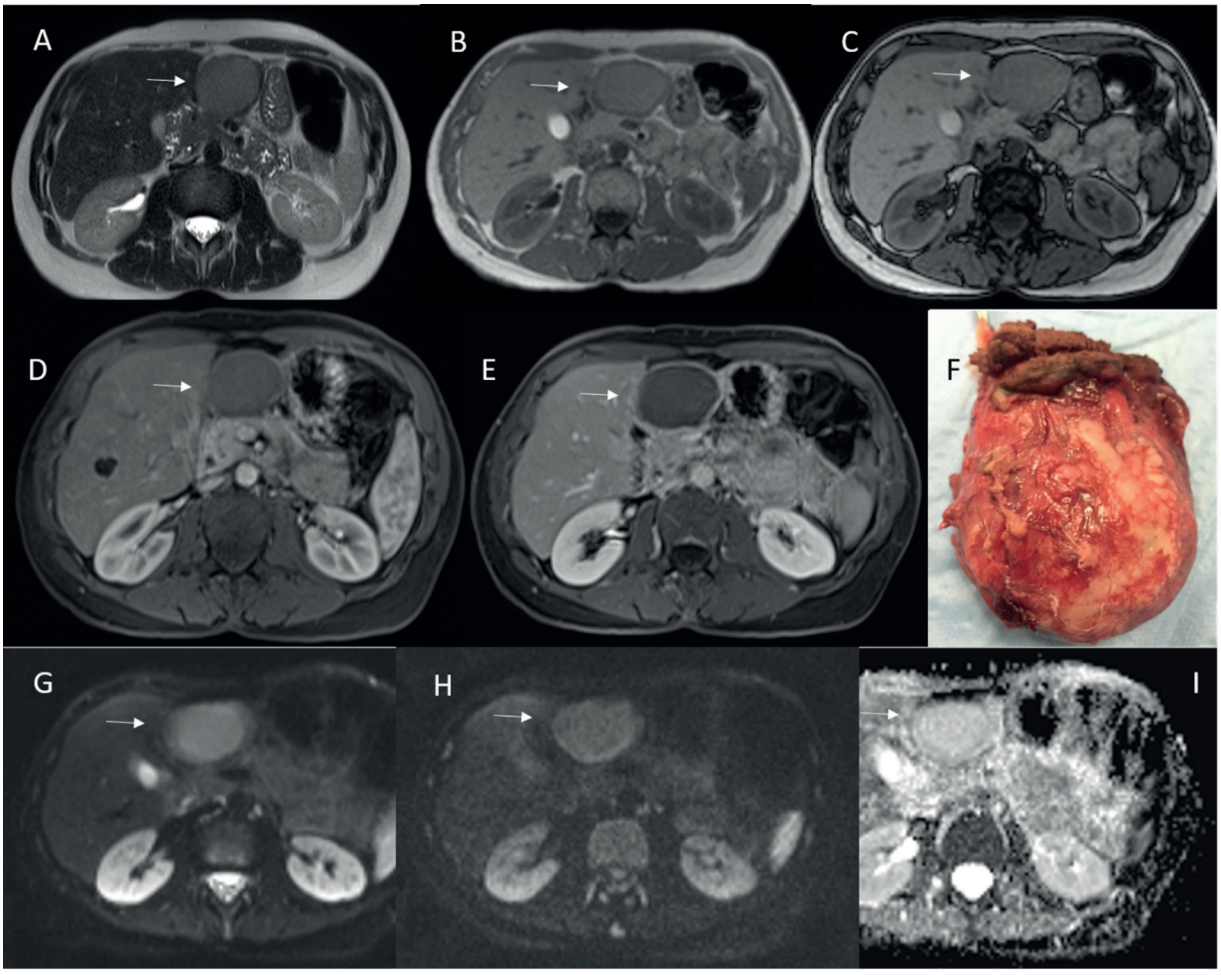

Figure 9. Cystoadenoma. The lesion shows hyperintense SI in T2-W (**A**), hypointense SI in T1-W sequences (**B**: in phase; **C**: out of phase) without contrast enhancement during arterial (**D**) and portal (**E**) phase and restricted diffusion (**G**: b50 s/mm^2; **H**: b 80 s/mm^2) and hyperintense SI in ADC map (**I**). in F it is shown specimen.

mance obtained by T2-W images and DWI, as we demonstrated in our previous study[30].

We found that LI-RADS is able to identify HCC lesions in non-cirrhotic liver. The reason is to be found in the fact that although these patients are classified as not at risk, all analyzed LI-RADS features have been implemented for HCC diagnosis.

Combined HCC-CCA is considered a rare entity of primary liver tumor consisting of mixed elements of HCC and CCA or cancer cells with hepatic progenitor/stem cell traits[12]. The cHCC-CCA incidence ranges from 1.0%-4.7% of all primary hepatic tumors[12]. In cHCC-CCA group we found that the more frequent radiological findings were suggestive of LR-M category. In fact, cHCC-CCAs showed inhomogeneous arterial contrast enhancement, with a peripheral rim during arterial phase and a progressive contrast enhancement, so as the presence of satellite nodules was a feature typical of cHCC-CC. According to our previous results, wash-out appearance was found in 54.5% of patients while the capsule appearance absence is more frequent (81.8%) in cHCC-CCA group compared to HCC group (37.2%). Therefore, the capsule appearance absence in nodule that shows peripheral and progressive CE should guide the radiologist in differential diagnosis, since these features are more specific for cHCC-CCA[12]. We found a high diagnostic accuracy (96.8%) to classify malignant and benign lesion, although we did not demonstrate significant difference in signal and CE appearance among all LR-M categories (p-value > 0.05). However, among LR-M categories the presence of satellite nodules was a feature typical of cHCC-CC, while the presence of intra lesion necrosis and hemorrhage was suggestive of sarcoma. Recent studies[39-42] of patients with solitary primary liver carcinomas found that

the LR-M category confers a worse post-surgical prognosis independent of actual pathologic diagnosis. This result raises the question of whether modifications to optimize the correlation of LI-RADS categories with pathologic diagnoses are even necessary. To this point, one must consider the possibility that revising the LR-M criteria to maximize sensitivity for non-HCC patients could further improve the ability of the LR-M category to predict worse patient outcomes.

The advantages related to the use of classifiers in the differential diagnosis between lesions are evident. So as the benefits related to the use of artificial intelligence (AI) systems that facilitate these processes are clear[43-45]. The major difficulties are related to the communication of the radiological findings to the referring clinicians. Radiology reports are traditionally created as non-structured free text (FRT) presentations in narrative language. However, inconsistencies regarding content, style, and presentation can hamper information transfer and diminish the reports clarity[46-51]. The resulting communication errors can lead to incorrect diagnosis, delayed initiation of adequate treatment, or adverse patient outcomes. Therefore, FRT should be organized and shifted toward structured reports (SR). The use of SR provides a checklist as to whether all relevant items for a particular radiological examination are addressed. Moreover, thanks to this "structure", the radiological report allows combining radiological data and other key clinical features, leading to a precise diagnosis and personalized medicine[51-55].

Conclusions

In this study, we found that LI-RADS showed a high diagnostic accuracy to classify malignant and benign lesion, although we did not demonstrate significant difference in signal and contrast enhancement appearance among all LR-M categories (p-value > 0.05). However, among LR-M

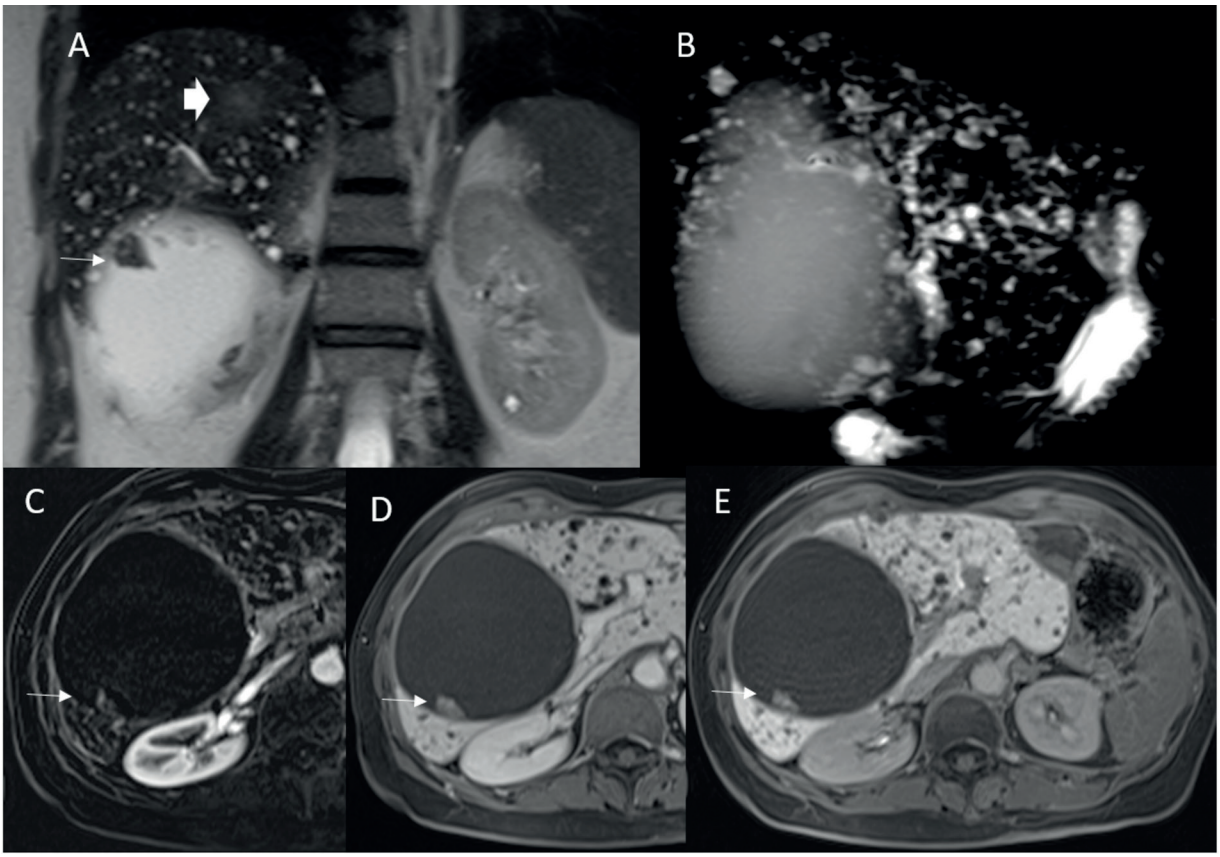

Figure 10. Cystoadenocarcinoma. The cystic component of the lesion is combined with a solid nodule, that is heterogeneously hyperintense in T2 W sequences (**A** and **B**) with a progressive contrast enhancement during the different phase of study (**C**: arterial; **D**: portal and **E**: HB phase).

categories the presence of ancillary features as satellite nodules or the presence of intra lesion necrosis and hemorrhage could help the radiologist towards a correct diagnosis. Therefore, it would be useful to analyse the LR-M category by implementing some considerations.

Author Contributions

Conceptualization, Vincenza Granata; Data curation, Vincenza Granata; Formal analysis, Vincenza Granata; Investigation, Vincenza Granata, Maria Luisa Barretta, Daniela Maria Iasevoli, Raffaele Palaia, Andrea Belli, Renato Patrone, Fabiana Tatangelo, Giulia Grazzini, Roberta Grassi, Francesca Grassi and Antonella Petrillo; Methodology, Vincenza Granata, Roberta Fusco, Sergio Venanzio Setola, Roberta Grassi, Alessandro Anselmo, Roberto Grassi, Francesco Izzo and Antonella Petrillo; Writing – original draft, Vincenza Granata; Writing – review and editing, Vincenza Granata and Roberta Fusco.

Conflicts of Interest

The authors declare no conflicts of interest.

Acknowledgements

The authors are grateful to Alessandra Trocino, librarian at the National Cancer Institute of Naples, Italy. Moreover, for the collaboration, authors are grateful to Paolo Pariante and Dr. Ivano Rossi, TSRM at Radiology Division, "Istituto Nazionale Tumori IRCCS Fondazione Pascale – IRCCS di Napoli", Naples, I-80131, Italy.

References

1) Global incidence and mortality of liver cancers and its relationship with the human development index (HDI): an ecology study in 2018 WCRJ 2019; 6: e1255.
2) Granata V, Fusco R, Maio F, Avallone A, Nasti G, Palaia R, Albino V, Grassi R, Izzo F, Petrillo A. Qualitative assessment of EOB-GD-DTPA and Gd-BT-DO3A MR contrast studies in HCC patients and colorectal liver metastases. Infect Agent Cancer 2019; 14: 40.
3) Granata V, Fusco R, Setola SV, Picone C, Vallone P, Belli A, Incollingo P, Albino V, Tatangelo F, Izzo F, Petrillo A. Microvascular invasion and grading in hepatocellular carcinoma: correlation with major and ancillary features according to LIRADS. Abdom Radiol (NY) 2019; 44: 2788-2800.
4) Li J, Cao B, Bi X, Chen W, Wang L, Du Z, Zhang X, Yu X. Evaluation of liver function in patients with chronic hepatitis B using Gd-EOB-DTPA-enhanced T1 mapping at different acquisition time points: a feasibility study. Radiol Med; 126: 1149-1158.
5) Esposito A, Buscarino V, Raciti D, Casiraghi E, Manini M, Biondetti P, Forzenigo L. Characterization of liver nodules in patients with chronic liver disease by MRI: performance of the Liver Imaging Reporting and Data System (LI-RADS v.2018) scale and its comparison with the Likert scale. Radiol Med 2020; 125: 15-23.
6) Gabelloni M, Di Nasso M, Morganti R, Faggioni L, Masi G, Falcone A, Neri E. Application of the ESR iGuide clinical decision support system to the imaging pathway of patients with hepatocellular carcinoma and cholangiocarcinoma: preliminary findings. Radiol Med 2020; 125: 531-537.
7) Barabino M, Gurgitano M, Fochesato C, Angileri SA, Franceschelli G, Santambrogio R, Mariani NM, Opocher E, Carrafiello G. LI-RADS to categorize liver nodules in patients at risk of HCC: tool or a gadget in daily practice? Radiol Med 2021; 126: 5-13.
8) Cholangiocarcinoma Working Group. Italian Clinical Practice Guidelines on Cholangiocarcinoma - Part I: Classification, diagnosis and staging. Dig Liver Dis 2020; 52: 1282-1293.
9) Cholangiocarcinoma Working Group. Italian Clinical Practice Guidelines on Cholangiocarcinoma - Part II: Treatment. Dig Liver Dis 2020; 52: 1430-1442.
10) Granata V, Fusco R, Amato DM, Albino V, Patrone R, Izzo F, Petrillo A. Beyond the vascular profile: conventional DWI, IVIM and kurtosis in the assessment of hepatocellular carcinoma. Eur Rev Med Pharmacol Sci 2020; 24: 7284-7293.
11) Nakamura Y, Higaki T, Honda Y, Tatsugami F, Tani C, Fukumoto W, Narita K, Kondo S, Akagi M, Awai K. Advanced CT techniques for assessing hepatocellular carcinoma. Radiol Med 2021; 126: 925-935.
12) Granata V, Fusco R, Venanzio Setola S, Sandomenico F, Luisa Barretta M, Belli A, Palaia R, Tatangelo F, Grassi R, Izzo F, Petrillo A. Major and ancillary features according to LI-RADS in the assessment of combined hepatocellular-cholangiocarcinoma. Radiol Oncol 2020; 54: 149-158.
13) Mathew RP, Sam M, Raubenheimer M, Patel V, Low G. Hepatic hemangiomas: the various imaging avatars and its mimickers. Radiol Med 2020; 125: 801-815.
14) Gatti M, Calandri M, Bergamasco L, Darvizeh F, Grazioli L, Inchingolo R, Ippolito D, Rousset S, Veltri A, Fonio P, Faletti R. Characterization of the arterial enhancement pattern of focal liver lesions by multiple arterial phase magnetic resonance imaging: comparison between hepatocellular carcinoma and focal nodular hyperplasia. Radiol Med 2020; 125: 348-355.
15) Cifrián Canales I, García Bernardo CM, Contreras Saiz E. Hepatic epithelioid hemangioendothelioma: a rare vascular tumor with unpredictable diagnosis. Rev Esp Enferm Dig 2021; 113: 300-301.
16) Gigante E, Paradis V, Ronot M, Cauchy F, Soubrane O, Ganne-Carrié N, Nault JC. New insi-

ghts into the pathophysiology and clinical care of rare primary liver cancers. JHEP Rep 2020; 3: 100174.

17) Granata V, Fusco R, Catalano O, Filice S, Avallone A, Piccirillo M, Leongito M, Palaia R, Grassi R, Izzo F, Petrillo A. Uncommon neoplasms of the biliary tract: radiological findings. Br J Radiol 2017; 90: 20160561.

18) Granata V, Fusco R, Avallone A, Cassata A, Palaia R, Delrio P, Grassi R, Tatangelo F, Grazzini G, Izzo F, Petrillo A. Abbreviated MRI protocol for colorectal liver metastases: How the radiologist could work in pre surgical setting. PLoS One 2020; 15: e0241431.

19) Granata V, Fusco R, de Lutio di Castelguidone E, Avallone A, Palaia R, Delrio P, Tatangelo F, Botti G, Grassi R, Izzo F, Petrillo A. Diagnostic performance of gadoxetic acid-enhanced liver MRI versus multidetector CT in the assessment of colorectal liver metastases compared to hepatic resection. BMC Gastroenterol 2019; 19: 129.

20) Izzo F, Granata V, Grassi R, Fusco R, Palaia R, Delrio P, Carrafiello G, Azoulay D, Petrillo A, Curley SA. Radiofrequency Ablation and Microwave Ablation in Liver Tumors: An Update. Oncologist 2019; 24: e990-e1005.

21) Marschner C, Zhang L, Schwarze V, Völckers W, Froelich MF, von Münchhausen N, Schnitzer ML, Geyer T, Fabritius MP, Rübenthaler J, Clevert DA. The diagnostic value of contrast-enhanced ultrasound (CEUS) for assessing hepatocellular carcinoma compared to histopathology; a retrospective single-center analysis of 119 patients. Clin Hemorheol Microcirc 2020; 76: 453-458.

22) Son JH, Choi SH, Kim SY, Lee SJ, Park SH, Kim KW, Won HJ, Shin YM, Kim PN. Accuracy of contrast-enhanced ultrasound liver imaging reporting and data system: a systematic review and meta-analysis. Hepatol Int 2020; 14: 1104-1113.

23) Mole DJ, Fallowfield JA, Sherif AE, Kendall T, Semple S, Kelly M, Ridgway G, Connell JJ, McGonigle J, Banerjee R, Brady JM, Zheng X, Hughes M, Neyton L, McClintock J, Tucker G, Nailon H, Patel D, Wackett A, Steven M, Welsh F, Rees M; HepaT1ca Study Group. Quantitative magnetic resonance imaging predicts individual future liver performance after liver resection for cancer. PLoS One 2020; 15: e 0238568.

24) Ai Z, Han Q, Huang Z, Wu J, Xiang Z. The value of multiparametric histogram features based on intravoxel incoherent motion diffusion-weighted imaging (IVIM-DWI) for the differential diagnosis of liver lesions. Ann Transl Med 2020; 8: 1128.

25) Esposito A, Buscarino V, Raciti D, Casiraghi E, Manini M, Biondetti P, Forzenigo L. Characterization of liver nodules in patients with chronic liver disease by MRI: performance of the Liver Imaging Reporting and Data System (LI-RADS v.2018) scale and its comparison with the Likert scale. Radiol Med 2020; 125: 15-23.

26) Argalia G, Tarantino G, Ventura C, Campioni D, Tagliati C, Guardati P, Kostandini A, Marzioni M, Giuseppetti GM, Giovagnoni A. Shear wave elastography and transient elastography in HCV patients after direct-acting antivirals. Radiol Med 2021; 126: 894-899.

27) Bozkurt M, Eldem G, Bozbulut UB, Bozkurt MF, Kılıçkap S, Peynircioğlu B, Çil B, Lay Ergün E, Volkan-Salanci B. Factors affecting the response to Y-90 microsphere therapy in the cholangiocarcinoma patients. Radiol Med 2021; 126: 323-333.

28) Danti G, Addeo G, Cozzi D, Maggialetti N, Lanzetta MM, Frezzetti G, Masserelli A, Pradella S, Giovagnoni A, Miele V. Relationship between diagnostic imaging features and prognostic outcomes in gastrointestinal stromal tumors (GIST). Acta Biomed 2019; 90: 9-19.

29) Granata V, Fusco R, Setola SV, Avallone A, Palaia R, Grassi R, Izzo F, Petrillo A. Radiological assessment of secondary biliary tree lesions: an update. J Int Med Res 2020; 48: 300060519850398.

30) Granata V, Fusco R, Catalano O, Avallone A, Palaia R, Botti G, Tatangelo F, Granata F, Cascella M, Izzo F, Petrillo A. Diagnostic accuracy of magnetic resonance, computed tomography and contrast enhanced ultrasound in radiological multimodality assessment of peribiliary liver metastases. PLoS One 2017; 12: e0179951.

31) Granata V, Fusco R, Catalano O, Avallone A, Leongito M, Izzo F, Petrillo A. Peribiliary liver metastases MR findings. Med Oncol 2017; 34: 124.

32) Granata V, Catalano O, Fusco R, Tatangelo F, Rega D, Nasti G, Avallone A, Piccirillo M, Izzo F, Petrillo A. The target sign in colorectal liver metastases: an atypical Gd-EOB-DTPA "uptake" on the hepatobiliary phase of MR imaging. Abdom Imaging 2015; 40: 2364-2371.

33) American College of Radiology. The LI-RADS v2018 Manual. American College of Radiology website. https://www.acr.org/-/media/ACR/Files/Clinical-Resources/LIRADS/LI-RADS-2018- Manual-5Dec18.pdf. Accessed June 2020.

34) American College of Radiology. The LI-RADS Lexicon. American College of Radiology website. https://www.acr.org/-/media/ACR/Files/RADS/LI-RADS/Lexicon-Table-2020.pdf. Accessed June 2020.

35) Cho MJ, An C, Aljoqiman KS, Choi JY, Lim JS, Park MS, Rhee H, Kim MJ. Diagnostic performance of Liver Imaging Reporting and Data System in patients at risk of both hepatocellular carcinoma and metastasis. Abdom Radiol (NY) 2020; 45: 3789-3799.

36) Ludwig DR, Fraum TJ, Cannella R, Tsai R, Naeem M, LeBlanc M, Salter A, Tsung A, Fleckenstein J, Shetty AS, Borhani AA, Furlan A, Fowler KJ. Expanding the Liver Imaging Reporting and Data System (LI-RADS) v2018 diagnostic population: performance and reliability of LI-RADS for distinguishing hepatocellular carcinoma (HCC) from non-HCC primary liver carcinoma in patients who do not meet strict LI-RADS high-risk criteria. HPB (Oxford) 2019; 21: 1697-1706.

37) Ludwig DR, Fraum TJ, Cannella R, Ballard DH, Tsai R, Naeem M, LeBlanc M, Salter A, Tsung A, Shetty AS, Borhani AA, Furlan A, Fowler KJ. Hepatocellular carcinoma (HCC) versus non-HCC: accuracy and reliability of Liver Imaging Reporting and Data System v2018. Abdom Radiol (NY) 2019; 44: 2116-2132.

38) Fraum TJ, Cannella R, Ludwig DR, Tsai R, Naeem M, LeBlanc M, Salter A, Tsung A, Shetty AS, Borhani AA, Furlan A, Fowler KJ. Assessment of primary liver carcinomas other than hepatocellular carcinoma (HCC) with LI-RADS v2018: comparison of the LI-RADS target population to patients without LI-RADS-defined HCC risk factors. Eur Radiol 2020; 30: 996-1007.

39) Kierans AS, Makkar J, Guniganti P, Cornman-Homonoff J, Lee MJ, Pittman M, Askin G, Hecht EM. Validation of Liver Imaging Reporting and Data System 2017 (LI-RADS) Criteria for Imaging Diagnosis of Hepatocellular Carcinoma. J Magn Reson Imaging 2019; 49: e205-e215.

40) Gonçalves DL, Leite JP, Silva R, Pissarra AP, Caetano Oliveira R, Silva D. Hepatic Adenomatosis: A Challenging Liver Disease. GE Port J Gastroenterol 2020; 27: 37-42.

41) Granata V, Fusco R, Setola SV, Castelguidone ELD, Camera L, Tafuto S, Avallone A, Belli A, Incollingo P, Palaia R, Izzo F, Petrillo A. The multidisciplinary team for gastroenteropancreatic neuroendocrine tumours: the radiologist's challenge. Radiol Oncol 2019; 53: 373-387.

42) Nardone V, Reginelli A, Guida C, Belfiore MP, Biondi M, Mormile M, Banci Buonamici F, Di Giorgio E, Spadafora M, Tini P, Grassi R, Pirtoli L, Correale P, Cappabianca S, Grassi R. Delta-radiomics increases multicentre reproducibility: a phantom study. Med Oncol 2020; 37: 38.

43) Berretta M, Cobellis G, Franco R, Panarese I, Rinaldi B, Nasti G, Di Francia R, Rinaldi L. Features of microvessel density (MVD) and angiogenesis inhibitors in therapeutic approach of hepatocellular carcinoma (HCC). Eur Rev Med Pharmacol Sci 2019; 23: 10139-10150.

44) Fiorini F, Granata A, Battaglia Y, Karaboue MAA. Talking about medicine through mass media. G Ital Nefrol 2019; 36: 2019-vol1.

45) Cantisani V, Iannetti G, Miele V, Grassi R, Karaboue M, Cesarano E, Vimercati F, Calliada F. Addendum to the sonographic medical act. J Ultrasound 2021; 24: 229-230.

46) Koc A, Sezgin OS, Kayipmaz S. Comparing different planimetric methods on volumetric estimations by using cone beam computed tomography. Radiol Med 2020; 125: 398-405.

47) Neri E, Miele V, Coppola F, Grassi R. Use of CT and artificial intelligence in suspected or COVID-19 positive patients: statement of the Italian Society of Medical and Interventional Radiology. Radiol Med 2020; 125: 505-508.

48) Granata V, Grassi R, Miele V, Larici AR, Sverzellati N, Cappabianca S, Brunese L, Maggialetti N, Borghesi A, Fusco R, Balbi M, Urraro F, Buccicardi D, Bortolotto C, Prost R, Rengo M, Baratella E, De Filippo M, Barresi C, Palmucci S, Busso M, Calandriello L, Sansone M, Neri E, Coppola F, Faggioni L. Structured Reporting of Lung Cancer Staging: A Consensus Proposal. Diagnostics (Basel) 2021; 11: 1569.

49) Wallis A, McCoubrie P. The radiology report—are we getting the message across? Clin Radiol 2011; 66: 1015-1022.

50) Bosmans JM, Peremans L, Menni M, De Schepper AM, Duyck PO, Parizel PM. Structured reporting: if, why, when, how-and at what expense? Results of a focus group meeting of radiology professionals from eight countries. Insights Imaging 2012; 3: 295-302.

51) Weiss DL, Langlotz CP. Structured reporting: patient care enhancement or productivity nightmare? Radiology 2008; 249: 739-747.

52) Granata V, Pradella S, Cozzi D, Fusco R, Faggioni L, Coppola F, Grassi R, Maggialetti N, Buccicardi D, Lacasella GV, Montella M, Ciaghi E, Bellifemine F, De Filippo M, Rengo M, Bortolotto C, Prost R, Barresi C, Cappabianca S, Brunese L, Neri E, Grassi R, Miele V. Computed Tomography Structured Reporting in the Staging of Lymphoma: A Delphi Consensus Proposal. J Clin Med 2021; 10: 4007.

53) European Society of Radiology (ESR). ESR paper on structured reporting in radiology. Insights Imaging 2018; 9: 1-7.

54) Granata V, Caruso D, Grassi R, Cappabianca S, Reginelli A, Rizzati R, Masselli G, Golfieri R, Rengo M, Regge D, Lo Re G, Pradella S, Fusco R, Faggioni L, Laghi A, Miele V, Neri E, Coppola F. Structured Reporting of Rectal Cancer Staging and Restaging: A Consensus Proposal. Cancers (Basel) 2021; 13: 2135.

55) Borghesi A, Sverzellati N, Polverosi R, Balbi M, Baratella E, Busso M, Calandriello L, Cortese G, Farchione A, Iezzi R, Palmucci S, Pulzato I, Rampinelli C, Romei C, Valentini A, Grassi R, Larici AR. Impact of the COVID-19 pandemic on the selection of chest imaging modalities and reporting systems: a survey of Italian radiologists. Radiol Med 2021; 1-15.